ENVIRONMENTAL STUDIES

When floods hit the road: Resilience to flood-related traffic disruption in the San Francisco Bay Area and beyond

Indraneel G. Kasmalkar[1]*, Katherine A. Serafin[2,3]*, Yufei Miao[4†], I. Avery Bick[4], Leonard Ortolano[4], Derek Ouyang[2], Jenny Suckale[1,2,4‡]

As sea level rises, urban traffic networks in low-lying coastal areas face increasing risks of flood disruptions. Closure of flooded roads causes employee absences and delays, creating cascading impacts to communities. We integrate a traffic model with flood maps that represent potential combinations of storm surges, tides, seasonal cycles, interannual anomalies driven by large-scale climate variability such as the El Niño Southern Oscillation, and sea level rise. When identifying inundated roads, we propose corrections for potential biases arising from model integration. Our results for the San Francisco Bay Area show that employee absences are limited to the homes and workplaces within the areas of inundation, while delays propagate far inland. Communities with limited availability of alternate roads experience long delays irrespective of their proximity to the areas of inundation. We show that metric reach, a measure of road network density, is a better proxy for delays than flood exposure.

INTRODUCTION

Global climate change is increasing the likelihood of extreme events (*1*) such as flooding, particularly in low-lying coastal areas (*2*). Rapid urbanization is further increasing flood risk, given the growing concentration of people and assets in cities and the clustering of cities along coastlines (*3*). Presently, about 50% of the world's population lives in cities, and the percentage is projected to rise to 68% by mid-century (*4*). This unprecedented urbanization is accompanied by rapid increases in the complexity and interconnectedness of physical human systems. Disruption of the highly interdependent socioeconomic networks through flooding and other hazards severely affects urban life, potentially leading to lasting displacement and business interruption (*5*). The indirect impacts associated with these disruptions could outweigh the direct impacts of flooding, which are defined as the physical damage to buildings and infrastructure.

The Intergovernmental Panel on Climate Change has emphasized the growing importance of indirect impacts but has also highlighted the challenges of quantifying indirect impacts (*5*). Challenges include the multitude of potential indirect impacts spanning the social, environmental, and economic spheres; the dependence on the cultural context; and the uncertainty surrounding the behavioral responses of individuals and communities. There also remains an open question of whether indirect impacts are governed primarily by the exposure to a climatic hazard or by the characteristics of the system experiencing disruption. These challenges raise questions about whether there are common themes to indirect climatic impacts that extend beyond the context of a specific hazard or location.

In this study, we move beyond a qualitative characterization of indirect impacts: We quantify the far-reaching traffic disruptions associated with coastal flooding in the San Francisco Bay Area over the next two decades, 2020–2040. For the purposes of this study, coastal flooding events are defined as extreme water levels resulting from various potential combinations of storm surges, tides, seasonal cycles, interannual anomalies driven by large-scale climate variability such as the El Niño Southern Oscillation, and sea level rise. We do not consider fluvial or pluvial flooding in our analysis but plan to integrate these processes in future work. To represent coastal flooding, we use 1-m resolution flood maps from the San Francisco Bay Conservation and Development Commission's Adapting to Rising Tides (ART) program (*6*).

The San Francisco Bay Area, similar to many other coastal regions, has dense urban development concentrated along its coastline. Thus, the region provides a valuable example for studying the indirect impacts of sea level rise and intensifying coastal floods on urban systems. This study is the result of a year-long service-learning course aimed at identifying actionable insights that advance the region's climate adaptation and planning efforts. We choose the traffic system as a starting point for understanding indirect impacts of climatic hazards since traffic systems connect the social, environmental, and economic dimensions of urban life. As in the San Francisco Bay Area, many urban traffic networks are already heavily congested. With a rising sea level, even relatively minor instances of coastal flooding could inundate major roads and lead to far-reaching, cascading consequences.

Traffic is highly nonlinear even under normal conditions, with congestion propagating rapidly from traffic bottlenecks to adjacent areas (*7*). However, not all traffic systems are equally prone to external disruptions, from flooding or otherwise (*8*, *9*). The varying responses of different traffic systems to disruptions has led to the concept of traffic resilience, which is defined as the ability of the traffic system to either withstand or recover from unexpected changes in traffic flows or road conditions (*8*). In this study, we define traffic resilience more specifically as the ability of the traffic system to mitigate travel time delays resulting from road closures. Recent studies on traffic resilience explore the role played by the structural and topological characteristics of the road network in reducing travel time delays (*9*, *10*). They suggest a variety of network flow–based metrics (*11*, *12*) and graph theoretic metrics (*13*, *14*) to estimate traffic resilience, but there is no consensus on a single metric (*15*).

While the characteristics of the road network are important, they alone do not dictate traffic resilience. Exposure to climatic hazards

[1]Institute for Computational and Mathematical Engineering, Stanford University, Stanford, CA, USA. [2]Department of Geophysics, Stanford University, Stanford, CA, USA. [3]Department of Geography, University of Florida, Gainesville, FL, USA. [4]Department of Civil and Environmental Engineering, Stanford University, Stanford, CA, USA.
*These authors contributed equally to this work.
†Present address: China International Capital Corporation, Shanghai, China.
‡Corresponding author. Email: jsuckale@stanford.edu

(*16*) and regional commute patterns (*17*) are important as well. To identify the interplay of factors that govern traffic resilience to coastal flooding, we simulate morning traffic flows in the San Francisco Bay Area under a range of water levels represented by the ART flood maps. We infer the origins and destinations of morning commutes from the Longitudinal Employer-Household Dynamics Origin-Destination Employment Statistics (LODES) dataset, prepared by the U.S. Census Bureau (*18*), assuming that present-day commute patterns remain approximately indicative of commutes in the near future, defined as 2020–2040. Integrating a traffic model with flood maps, while not without its challenges (*13*, *19*), enables us to quantify how flood exposure, regional commute patterns, and characteristics of the road network affect traffic resilience.

METHODS

We integrate a fixed-demand incremental traffic assignment model with the ART flood maps to simulate regional traffic patterns in the San Francisco Bay Area in the presence of coastal flooding. The incremental traffic assignment model represents commuters as agents whose goal is to minimize their origin-destination travel time (*20*, *21*). Individual commuters are partitioned uniformly and proportionally into four sequential batches of sizes 40, 30, 20, and 10%, and commuters within each successive batch are assigned incrementally to their shortest-time origin-destination routes (*20*). This incremental approach incorporates the effects of the route choices of earlier commuters on the route choices of later commuters within a given time period (*20*, *21*). The collective route choice of commuters creates congestion and leads to increases in travel time on road segments, which are modeled with the widely used Bureau of Public Roads function (*20*).

The traffic assignment model requires two inputs: a road network model, and origin-destination commuter data. For the San Francisco Bay Area (Fig. 1A), we use the regional road network model developed by the Metropolitan Transportation Commission (MTC) (*22*) as the first input. The MTC road network, shown in Fig. 1B, is the basis of traffic simulations for regional planning in the San Francisco Bay Area (*23*). The MTC road network is a simplified version of the true road network. While it contains all the primary and secondary roads, it aggregates tertiary and local roads into simplified road segment representations to make traffic simulations computationally tractable. The MTC road network does not represent toll stations, carpool or express lanes, or traffic signals.

The LODES dataset (*18*) provides the second input to the traffic assignment model. It is an annually updated synthetic dataset that relies on census data, American Community Survey data, and data collected by state governments. The LODES dataset provides the number of employees who reside in a given census block and work in a given census block. We assume that the dataset represents pairs of origins and destinations for weekday morning commutes. We also assume that the present-day travel patterns described in the dataset resemble the travel patterns throughout the 2020–2040 time period. The LODES dataset does not present commute data by mode or time of commute. To match the scope of our study, we process the dataset using estimates from the American Community Survey (*24*) for the number of morning peak-hour commuters by cars and carpools for each origin-destination pair.

The use of the LODES dataset limits the spatial resolution of our model to the scale of census blocks that range from 100 m to 10 km in length (*25*). Most traffic analyses, on the other hand, are conducted on traffic analysis zones that range from 1 to 50 km in length (*19*, *23*). The smaller sizes of census blocks provide higher spatial resolution than the traffic analysis zones. We assume that any errors in the model at scales smaller than census block lengths, such as the errors resulting from local road aggregation within the simplified road network, are negligible at the spatial scale of census blocks.

To identify inundated roads, we overlay the MTC road network with the ART flood maps (*6*), as shown in Fig. 1 (C and D). The ART flood maps are 1-m resolution maps that represent water levels resulting from potential combinations of storm surges, tides, seasonal cycles, interannual anomalies driven by large-scale climate variability such as the El Niño Southern Oscillation, and sea level rise. The flood maps are designed with a "one map, many futures" approach, where the water level in each map represents multiple underlying sea level rise scenarios combined with extreme water level events. For example, the 36-inch water level represents both a 50-year extreme

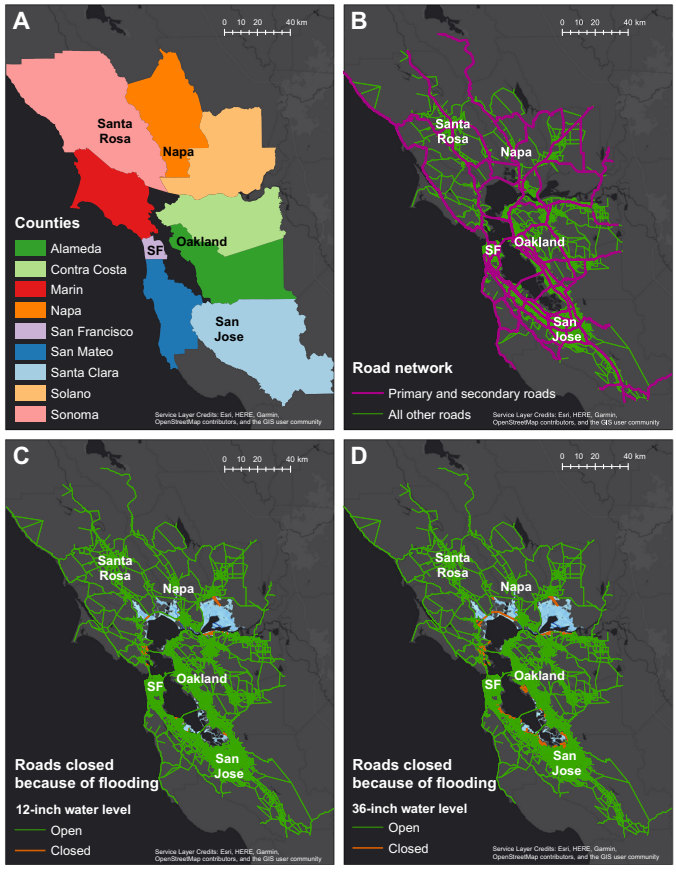

Fig. 1. The San Francisco Bay Area study site. (**A**) The nine counties of the San Francisco Bay Area. The cities of Santa Rosa, Napa, San Francisco (labeled SF), Oakland, and San Jose are shown for reference. The North Bay includes Napa, Marin, Sonoma, and Solano counties, depicted in orange and red; the East Bay includes Alameda and Contra Costa counties, depicted in green, and the South Bay and Peninsula include Santa Clara, San Mateo, and San Francisco counties, depicted in blue and purple. (**B**) The regional road network used in our model. Numbered roads (primary and secondary roads) are shown in magenta. (**C**) The flood map for the 12-inch water level overlying the road network. (**D**) The flood map for the 36-inch water level overlying the road network. In both (C) and (D), the areas of inundation are shown in blue, while the roads closed because of flooding are shown in red.

water level event at the present-day sea level and an approximately 20-year extreme water level event with 6 inches of sea level rise (*6*). By considering water levels rather than specific scenarios of flood intensities and sea level rise, the one map, many futures approach allows us to study a wide range of plausible coastal flooding events despite the uncertainty in projections of near-future sea level rise.

We consider four water levels in our analysis: the baseline "no flood," which represents no flooding at present-day sea level, and the 12-, 24-, and 36-inch water levels. Our choice of water levels is limited to coastal flood events with return periods of up to 50 years and sea level rise of up to 6 inches (see table S1 for more details), which are plausible ranges for the region for the 2020–2040 period (*6*, *26*, *27*). We do not consider water levels above 36 inches since the potential commutes under extreme water levels may not represent home-to-workplace commutes as assumed in the model. For example, a substantial number of commuters may change their objectives from work commute to evacuation for sufficiently extreme water levels. The ART flood maps do not consider the presence of buildings, underground spaces, or storm drainage systems and do not include fluvial or pluvial flooding. Additional details about the ART flood mapping methodology are provided in the Supplementary Materials.

We assume that road segments are closed to traffic flow if they exceed a certain threshold of inundation depth. The National Weather Service highlights 6 inches of inundation as posing a threat to individuals and 12 inches as sufficient to sweep most cars off the road (*28*). The decisions for road closures are made by local and regional authorities on the basis of local road conditions, creating a wide range of potential thresholds for road closures. However, our sensitivity tests over the range 1 to 12 inches for the road closure threshold show no noticeable change in our model results for the San Francisco Bay Area (fig. S1). For the purposes of this study, we choose the road closure threshold to be 3 inches. For road segments with less than 3 inches of flooding, the model increases the travel time on those segments according to an empirical relationship between inundation depth and maximum safe driving speed (*29*). The model then assigns commuters to routes on the altered road network.

As a result of road closures, certain home-workplace pairs may not have viable routes. If either the home or the workplace of the commuter is flooded, then the commute is not possible. Even if neither the home nor the workplace is flooded, strategic roads between the home and the workplace may have been closed, making the commute impossible. In the event that there is no accessible home-to-workplace route for a given commuter, that particular commute is classified as impassable. We assume that a commuter with an impassable commute stays at home and is not assigned to any route, leading to employee absences.

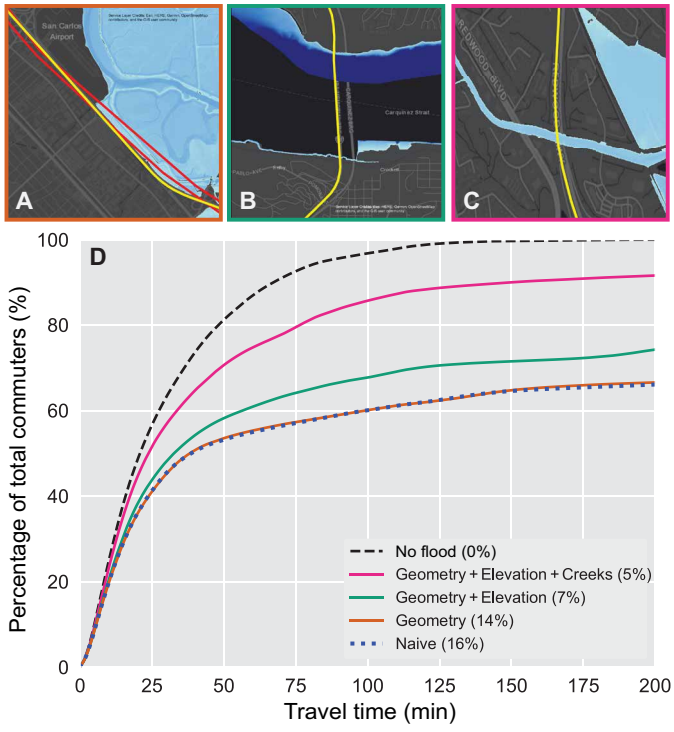

Fig. 2. The effects of model corrections on estimations of regional travel time delays. Model corrections were introduced during dataset integration to reduce biases in the process of identifying inundated roads. (**A**) Geometry correction, which represents the correction of the location and curvature of the primary and secondary roads. (A) shows a portion of U.S. 101 curving around the flooded region, in yellow, and the original, simplified straight-line road geometry intersecting the flood map, in red. (**B**) Elevation correction, which represents the incorporation of the primary and secondary road elevations above the ground. (B) shows the Carquinez Bridge elevated above the inundated region for the 36-inch water level. (**C**) Creek correction. A road segment is considered flooded if more than 17% of its length is flooded. (C) shows how the creek correction applies to the case of incorrect flooding for the U.S. 101 as it crosses the San Rafael Creek. (**D**) Cumulative distribution of travel time for commuters across the San Francisco Bay Area for the 36-inch water level computed with the various corrections. The naive approach, shown with a dotted line for easier distinction, represents overlaying the flood map on the road network with no corrections. The data inside the parentheses in the legend indicate the percentage of impassable commutes for a given water level.

Correcting model biases when identifying inundated roads

Traffic models simplify road networks (*23*) in ways that introduce potential biases when estimating flood impacts. In Fig. 2, we summarize the impact of three biases, labeled as "geometry," "elevation," and "creeks," on flood-related traffic disruption. The combination of the corrections for geometry, elevation, and creeks reduces travel times by 20 to 30% over the no-correction "naive" approach for all commuters for the 36-inch water level, as seen in Fig. 2D. The percentage of impassable commutes is similarly reduced from 16 to 5%.

The first bias arises from the representation of road segments as straight edges (*23*), which may incorrectly intersect the areas of inundation (Fig. 2A). To correct for this bias, we align the primary and secondary roads in the MTC road network with those of the true road network, where the latter network is obtained from a federal roadway dataset (*25*). Tertiary and local roads are not realigned in the same way since most of these road segments within the MTC road network are simplified and aggregated versions of the true roads.

The lack of elevation data in road networks introduces a second bias arising from the incorrect flooding of bridges and overpasses. We compute the above-ground elevation for primary and secondary roads using a Caltrans Global Positioning System–based elevation dataset (*30*) and a topography dataset (*31*) and reassess the inundation of these road segments. The elevation correction notably reduces projected travel time delays, as seen in Fig. 2D.

The incorrect flooding of road segments crossing over small creeks leads to a third bias. The topography of creek-road intersections is

often simplified in the digital elevation models of flood maps to allow for continuity in the flood mapping upstream of the intersections (*6*). Since creeks are substantially narrower than road segments, we correct for this bias by assuming that road segments are inundated only if the fraction of the segment length covered by water exceeds a certain threshold, which we call the water-cover threshold. We derive the threshold value as 17% by identifying anomalous peaks in the distribution over all road segments of the fraction of segment length covered by water (fig. S2).

RESULTS

Impassable or delayed commutes? Two types of flood-related disruption

Our model highlights two ways in which flooding can disrupt traffic flow. The closure of inundated roads makes certain routes impassable. We assume that commuters with impassable commutes stay home and are thus absent from their workplace. Road closures also force some commuters onto alternate roads, thus aggravating congestion on those roads and creating travel time delays. In the interest of simplicity, we assume that commuters with passable commutes continue toward their destination regardless of how long they are delayed.

We summarize how commuters throughout the San Francisco Bay Area experience flood-related traffic disruptions for the different water levels in Fig. 3. We consider a travel time delay of more than 30 min a substantial delay because 30 min is the average travel time for the San Francisco Bay Area in our model when there is no flood. As seen in Fig. 3A, the percentage of total commuters delayed by more than 30 min is much larger than the percentage of total commuters having an impassable commute for all water levels. Our model thus projects that travel time delays affect a substantially larger number of commuters than impassibility.

The magnitude of travel time delays also increases with water level, as seen in Fig. 3B, which shows the cumulative percentage of commuters by projected travel time. For example, while travel times are almost identical for the 12- and 24-inch water levels, there is a sharp increase in travel times for the 36-inch water level. These travel time delays are not equally distributed. Commuters with short commutes of 15 min or less experience negligible delays (Fig. 3B). In contrast, commuters who live far from their workplaces may be delayed substantially during coastal flood events.

Delays are experienced broadly over the entire region but with varying spatial extents. In Fig. 4, we show the percentage of commuters delayed over 30 min for the 12-inch water level (Fig. 4, A and C) and the 36-inch water level (Fig. 4, B and D). The top two panels (Fig. 4, A and B) aggregate the delayed commuters by their home census tracts, while the bottom two panels (Fig. 4, C and D) aggregate the delayed commuters by their workplace census tracts. We project the largest delays in Marin County, which has high flood exposure (*32*). However, delays also extend far beyond the areas of inundation, especially as the water level increases (Fig. 4, B and D).

In contrast, most impassible commutes are a result of either the home (Fig. 5, A and B) or the workplace (Fig. 5, C and D) being located within the areas of inundation. We present the spatial distribution of impassable commutes for the 12- and 36-inch water levels in Fig. 5. Census tracts where more than 50% of commutes are impassable, shown in dark blue, are mostly concentrated along the shoreline of the Bay.

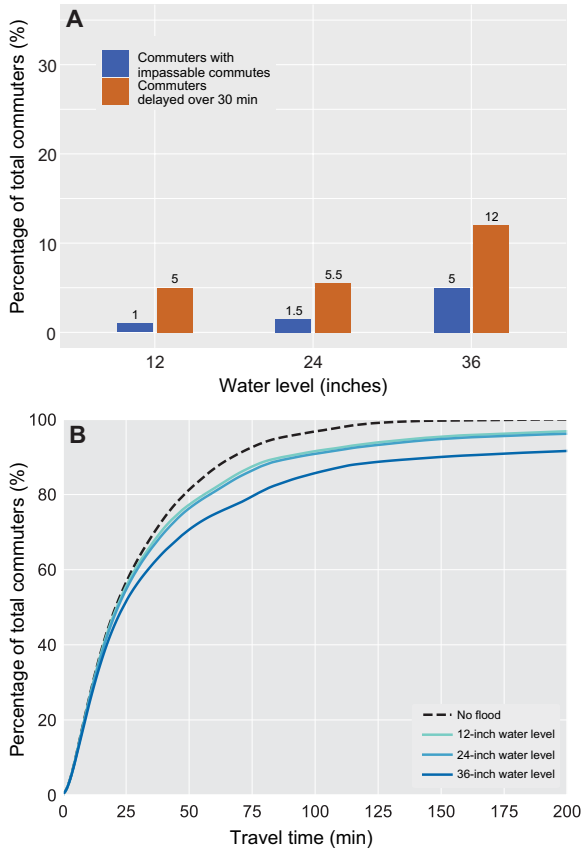

Fig. 3. Impassable commutes and travel time delays for all commuters. (**A**) Bar plot of the percentages of commuters experiencing impassable commutes and travel time delays exceeding 30 min for every water level. (**B**) The cumulative percentage of all commuters and their projected travel times for every water level.

Floods aggravate the congestion resulting from regional jobs-housing imbalances

Urban areas around the world have experienced sprawl through a confluence of factors such as population growth, land use decisions, and the development of transportation infrastructure (*33*). In particular, the rise in housing prices around urban centers and the availability of highways have resulted in housing and employment patterns that lead to heavy congestion and long travel times on major traffic routes (*34*). The potential flooding of these routes may amplify the already long travel times.

The San Francisco Bay Area consists of three broad regions: The South Bay and Peninsula, the North Bay, and the East Bay (Fig. 1A). The South Bay and Peninsula region is home to the economically thriving Silicon Valley, which has a robust job market with a surplus of high-paying jobs (*35*) but is known for its housing shortage (*36*). The North Bay and East Bay regions, in contrast, have greater availability of affordable housing (*36*). Consequently, a substantial percentage of residents of both the North Bay (17%; table S2) and the East Bay (33%; table S2) work in the South Bay and Peninsula.

The San Francisco Bay Area has strategic traffic corridors that connect the different regions. There are two potential causes of flood-related travel time delays arising along the main traffic corridors. First, the flooding and closure of traffic corridors located close to the Bay diverts commuters onto nearby local roads and highways,

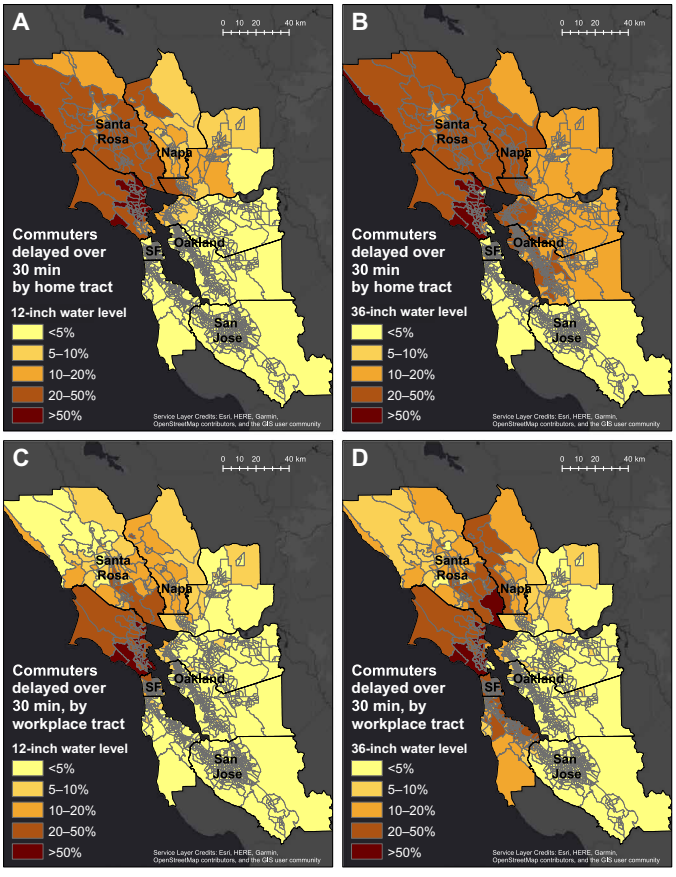

Fig. 4. Percentage of commuters experiencing more than 30 min of delays for 12- and 36-inch water levels, aggregated to census tracts. (**A**) Commuters by home tract for the 12-inch water level. (**B**) Same as (A), for the 36-inch water level. (**C**) Commuters by workplace tract for the 12-inch water level. (**D**) Same as (C), for the 36-inch water level. County borders are shown in black.

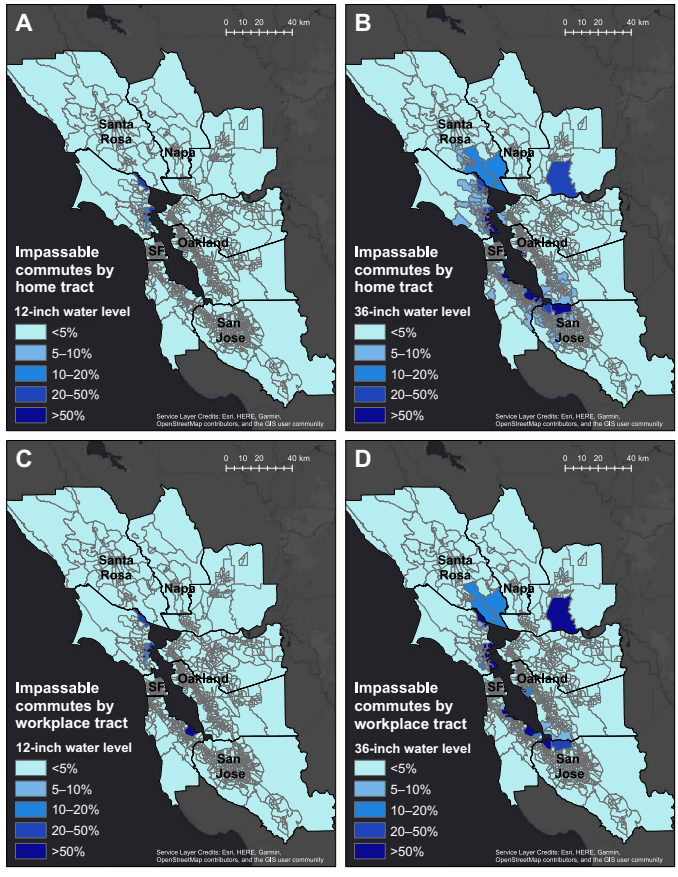

Fig. 5. Impassable commutes in the San Francisco Bay Area, aggregated to census tract. A tract with a dark blue color indicates that more than 50% of commuters whose home or workplace is located within the tract are unable to commute to their workplace as a result of flooding. (**A**) By home tract, 12-inch water level. (**B**) By home tract, 36-inch water level. (**C**) By workplace tract, 12-inch water level. (**D**) By workplace tract, 36-inch water level. County borders are shown in black.

thus increasing congestion and associated travel time delays on alternate routes. An example is the U.S. 101, which connects the North Bay with the South Bay and Peninsula and runs along the west shoreline of the Bay. Second, the San Francisco Bay Area has a number of bridges, such as the Dumbarton Bridge and the San Mateo Bridge, which run across the Bay and have low-lying entry roads. Flood-related closures of the entry roads force commuters to either choose a different bridge or drive around the Bay, adding to travel time delays.

The residents of the South Bay and Peninsula, the surplus job region, face minimal delays. A high percentage (87%; table S2) of South Bay and Peninsula residents work within the same region. The residents have multiple choices of traffic corridors to commute from home to work, not all of which are exposed to flooding. As seen in Fig. 4 (A and B), this region has a very low percentage (<5%) of residents who face delays of 30 min or more for the 12- and 36-inch water levels.

The distribution of projected flood-related travel time delays in Fig. 4 reflects the asymmetry of the jobs-housing imbalance. A large percentage of East Bay residents (33%; table S2) work in the South Bay and Peninsula. East Bay residents face large delays, while the South Bay and Peninsula residents face minimal delays (Fig. 4B). In contrast, East Bay workplaces experience minimal delays, unlike the South Bay and Peninsula workplaces (Fig. 4D). These results suggest that regional jobs-housing imbalances are preexisting vulnerabilities in the traffic system that may trigger additional flood-related travel time delays.

Characteristics of the road network govern traffic resilience to flood-related delays

Previous studies of traffic resilience (*8*–*10*, *13*) highlight that redundancy, defined as the availability of alternate roads in a road network, can offset travel time delays resulting from road closures. Current metrics of redundancy are relatively computationally intensive since they use traffic flow simulations to quantify the impact of closing individual road segments (*11*, *12*). Other proposed proxies for traffic resilience include graph theoretic metrics such as betweenness centrality (*13*, *37*, *38*), which measures how "central" road segments are for traffic flow. These metrics, however, are not ideal proxies for traffic resilience because they do not capture the possibility of substitution. For example, betweenness centrality does not distinguish between widely used traffic corridors such as U.S. 101 that traverse through dense urban areas and fairly isolated highways with limited

alternatives such as State Route 1. Local roads are available in the former case to partially offset a closure of the major traffic corridor but not in the latter.

We present an alternate, simple graph theoretic metric, metric reach (*39*), and demonstrate its negative correlation with travel time delays. The metric reach of a road segment is defined as the number of unique road miles that can be covered starting from that segment within a service radius (*39*). The average metric reach of a region correlates strongly with road network density, namely, the total street length per square mile, as well as the total number of intersections per square mile (*39*). These correlations suggest that metric reach has the potential to approximate the availability of alternate roads within a given region. For all metric reach calculations in this study, we set the service radius parameter to 5 miles. Sensitivity tests of metric reach show no noticeable relative change for service radii of 5, 10, 15, and 20 miles.

Figure 6 explores the explanatory potential of metric reach for understanding traffic resilience to coastal flooding in the San Francisco Bay Area. Figure 6A is a map of the average metric reach for each county in the San Francisco Bay Area. In particular, Fig. 6A shows that counties in the North Bay have lower metric reach than the other counties. In Fig. 6B, we compare the average travel time delay per mile, shown by marker size, with the average metric reach and the percentage of road capacity flooded for each county, for the 36-inch water level. Marin County, in the North Bay, stands out for having both the largest delays and the highest flooded road capacity (14.5%; table S3). The other counties in the North Bay, Napa, Sonoma, and Solano also experience some of the largest delays even with relatively low flooded road capacities.

To identify the comparative influence of metric reach and percentage of flooded road capacity on the average delays per mile for the nine counties, we perform a log-transformed linear regression of these metrics for the 36-inch water level (table S4). Our analysis shows strong correlation (R^2 = 0.86; table S4) with average delay per mile.

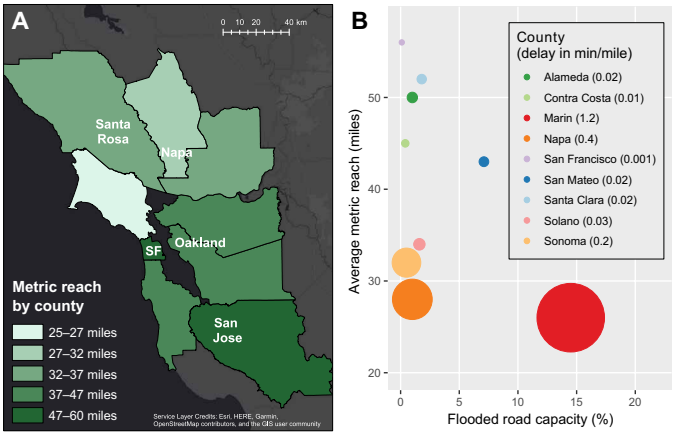

Fig. 6. Metric reach versus travel time delays. (**A**) The metric reach averaged over the road subnetwork of each county. Metric reach represents the road network density for a given region. It is computed with a service radius of 5 miles. (**B**) The average delay for the 36-inch water level for every county against its percentage of flooded road capacity and its average metric reach. Colors indicate the different counties, while the sizes of the circles represent the average travel time delay in min/mile. Marin County, shown as the largest red circle, has the highest average delay, the largest flooded road capacity, and the lowest metric reach of all counties in the San Francisco Bay Area. The underlying data for (B) are provided in table S3.

Assuming a significance threshold of $\alpha = 0.05$, the regression indicates that the averaged metric reach is statistically significant (P value = 0.003; table S4), while the percentage of flooded road capacity is not significant (P value = 0.259; table S4). Thus, the analysis indicates that the metric reach of a region predicts delays better than flood exposure. Regression analyses of metric reach and travel time delays also yield strong correlations for the 12-inch (R^2 = 0.80; table S5) and 24-inch (R^2 = 0.86; table S5) water levels.

The ART flood maps project that San Mateo County will experience extensive flooding in the near future (*6*), but this flooding may not translate into travel time delays to the degree that one might expect on the basis of exposure. The county, shown in dark blue in Fig. 6B, has the second largest percentage of road capacity flooded in the 36-inch water level (7%; table S3). However, our model projects low average delay per mile (0.02 min/mile; table S3). Our analysis suggests that high metric reach reduces the projected delays in San Mateo County. However, the county experiences a relatively large percentage of impassable commutes (13%; table S3) as a result of its high flood exposure.

Discussion of implications beyond the San Francisco Bay Area

Our study of flood-related traffic disruption highlights the far-reaching, indirect impacts of climatic hazards on urban systems. We identify two types of disruption to traffic networks as a result of coastal flooding: (i) the emergence of impassable commutes when origin, destination, or critical road connections fall into the areas of inundation and (ii) travel time delays that spread throughout the entire regional network irrespective of proximity to the areas of inundation. These two disruptions, namely, the absence and delay of employees, have consequences for both the individual employees and businesses and for the broader regional economy.

Different factors govern the dynamics of these two types of disruption. Flood exposure of homes and workplaces largely determines impassability. In contrast, flood exposure is a poor predictor of travel time delays. Our model projects the largest delays in regions with low metric reach since these regions have limited availability of alternate roads to offset disrupted traffic. The regions with low metric reach may experience delays irrespective of their proximity to the areas of inundation. Travel time delays hence propagate region-wide, and they affect a much larger percentage of commuters than impassability does (Fig. 3B). Therefore, the common assumption that floods only affect a seemingly small number of communities within the areas of inundation is questionable and could undermine planning efforts dedicated to advancing community well-being and regional competitiveness.

The dynamics of flood-related traffic disruption highlighted in this study can provide valuable insights for coastal regions beyond the San Francisco Bay Area. Many regions around the world share common characteristics with the San Francisco Bay Area such as dense urban development along the coastline and highly congested traffic networks. However, the San Francisco Bay Area has a unique geography. The traffic patterns that arise from the geography may introduce special vulnerabilities associated with flooding. Many major traffic corridors line the shoreline and two bridges with low-lying entry roads connect the South Bay and Peninsula to the East Bay (Fig. 1B). These particular traffic corridors and bridges act as nexus points for traffic congestion, even in the absence of hazards (*23*) as also demonstrated in a recent comparison of delays due to road closures in different U.S. cities (*9*).

Apart from differences in geography and traffic patterns, some of the assumptions within our traffic model may not apply in other coastal regions. For example, we assume that commuters have complete knowledge of flood conditions, which enables them to identify their shortest-time viable routes before commencing their journeys. The assumption is reasonable for the San Francisco Bay Area given the prevalence of mobile traffic applications but may not generalize to regions in other parts of the world. Similarly, we do not currently consider public transport or biking in our model, which could be a limitation in urban areas where those modes of transport are common.

Even for regions where the assumptions of our model are applicable, performing traffic simulations may prove difficult because of the lack of appropriate datasets. Not all regions have commuter origin-destination datasets, representations of the regional road network suitable for traffic modeling, or the additional datasets of road geometry and elevation needed to correct biases in model integration. To facilitate the analysis of traffic disruption resulting from climatic hazards in other regions, we propose using metric reach as a simple proxy for assessing traffic resilience within sufficiently large regions such as counties (tables S4, S5, and S6). Since metric reach is independent of the hazard that causes the closure of roads, our results suggest that the impact of different climatic hazards on travel time delays might not be as different as the hazards themselves. Accordingly, we suggest that other hazards, such as wildfires or hurricanes, would also primarily cause delays in regions with low metric reach. However, we emphasize that our model does not consider behavioral changes such as evacuations, which may substantially alter traffic patterns under conditions of high hazard severity.

While we do not consider behavioral changes specifically, our study implicitly demonstrates the potential value of changes in commute behavior. An ambitious reduction of commutes between homes and workplaces would not only reduce greenhouse gas emissions but also synergistically reduce the adverse impacts of coastal flooding, highlighting the potential cobenefits of climate change mitigation and adaptation. New technologies such as autonomous vehicles or telecommuting in conjunction with policies encouraging urban densification and public transit could help change commute patterns and achieve both adaptation and mitigation goals. Quantitative models that assess the impacts of climatic hazards on urban systems, such as the one in this study, enable an evaluation of the potential benefits of such technological and social transformations.

CONCLUSIONS

Our analysis quantifies one of the cascading, indirect consequences of present-day and near-future sea level rise: the disruption of urban traffic flows. We find a spectrum of indirect impacts of coastal flooding on traffic systems, from impassable commutes for communities in the areas of inundation to travel time delays that propagate regionwide. Our model suggests that communities with low metric reach are prone to experiencing long travel time delays since they do not have sufficiently many alternate roads to fully offset road closures. Thus, communities with low flood exposure may have similar or higher vulnerability to delays compared to those with high exposure depending on the nature of the local road network. Our finding demonstrates that the characteristics of an urban system can play a bigger role in the indirect impacts of hazards on the urban system than the exposure to the hazard. Since metric reach, a general characteristic of the traffic network, is independent of the hazard type, we suggest that metric reach may help identify regions prone to delays caused by other hazards.

SUPPLEMENTARY MATERIALS

Supplementary material for this article is available at http://advances.sciencemag.org/cgi/content/full/6/32/eaba2423/DC1

REFERENCES AND NOTES

1. S. I. Seneviratne, N. Nicholls, D. Easterling, C. M. Goodness, S. Kanae, J. Kossin, Y. Luo, J. Marenggo, K. McInnes, M. Rahimi, M. Reichstein, A. Sorteberg, C. Vera, X. Zhang, Chapter 3. Changes in Climate Extremes and their Impacts on the Natural Physical Environment, in *Managing the risks of extreme events and disasters to advance climate change adaptation. A Special Report of Working Groups I and II of the Intergovernmental Panel on Climate Change (IPCC)*, C. B. Field, V. R. Barros, D. J. Dokken, K. J. Mach, M. D. Mastrandrea, T. E. Bilir, M. Chatterjee, K. L. Ebi, Y. O. Estrada, R. C. Genova, B. Girma, E. S. Kissel, A. N. Levy, S. MacCracken, P. R. Mastrandrea, L. L. White, Eds. (Cambridge Univ. Press, 2012), pp. 109–230.
2. P. P. Wong, I. J. Losada, J. P. Gattuso, J. Hinkel, A. Khattabi, K. L. McInnes, Y. Saito, A. Sallenger, Chapter 5. Coastal systems and low-lying areas, in *Climate Change 2014: Impacts, Adaption and Vulnerability. Part A: Global and Sectoral Aspects. Contribution of Working Group II to the Fifth Assessment Report of the Intergovernmental Panel on Climate Change*, C. B. Field, V. R. Barros, D. J. Dokken, K. J. Mach, M. D. Mastrandrea, T. E. Bilir, M. Chatterjee, K. L. Ebi, Y. O. Estrada, R. C. Genova, B. Girma, E. S. Kissel, A. N. Levy, S. MacCracken, P. R. Mastrandrea, L. L. White, Eds. (Cambridge Univ. Press, 2014), pp. 361–409.
3. A. Revi, D. E. Satterthwaite, F. Aragón-Durand, J. Corfee-Morlot, R. B. R. Kiunsi, M. Pelling, D. C. Roberts, W. Solecki, Chapter 8. Urban Areas, in *Climate Change 2014: Impacts, Adaptation, and Vulnerability. Part A: Global and Sectoral Aspects. Contribution of Working Group II to the Fifth Assessment Report of the Intergovernmental Panel on Climate Change*, C. B. Field, V. R. Barros, D. J. Dokken, K. J. Mach, M. D. Mastrandrea, T. E. Bilir, M. Chatterjee, K. L. Ebi, Y. O. Estrada, R. C. Genova, B. Girma, E. S. Kissel, A. N. Levy, S. MacCracken, P. R. Mastrandrea, L. L. White, Eds. (Cambridge Univ. Press, 2014), pp. 535–612.
4. United Nations Population Division, "World Urbanization Prospects: The 2018 Revision" (2018).
5. M. Oppenheimer, M. Campos, R. Warren, J. Birkmann, G. Luber, B. O'Neill, K. Takahashi, Chapter 19. Emergent Risks and Key Vulnerabilities, in *Climate Change 2014: Impacts, Adaptation, and Vulnerability. Part A: Global and Sectoral Aspects. Contribution of Working Group II to the Fifth Assessment Report of the Intergovernmental Panel on Climate Change*, C. B. Field, V. R. Barros, D. J. Dokken, K. J. Mach, M. D. Mastrandrea, T. E. Bilir, M. Chatterjee, K. L. Ebi, Y. O. Estrada, R. C. Genova, B. Girma, E. S. Kissel, A. N. Levy, S. MacCracken, P. R. Mastrandrea, L. L. White, Eds. (Cambridge Univ. Press, 2014), pp. 1039–1099.
6. J. Vandever, M. Lightner, S. Kassem, J. Guyenet, M. Mak, C. Bonham-Carter, Adapting to Rising Tides Bay Area Sea Level Rise Analysis and Mapping Project (2017); www.adaptingtorisingtides.org/wp-content/uploads/2018/07/BATA-ART-SLR-Analysis-and-Mapping-Report-Final-20170908.pdf.
7. B. S. Kerner, *The Physics of Traffic: Empirical Freeway Pattern Features, Engineering Applications, and Theory* (Springer, 2012).
8. D. Freckleton, K. Heaslip, W. Louisell, J. Collura, Evaluation of resiliency of transportation networks after disasters. *Transp. Res. Rec.* **2284**, 109–116 (2012).
9. A. A. Ganin, M. Kitsak, D. Marchese, J. M. Keisler, T. Seager, I. Linkov, Resilience and efficiency in transportation networks. *Sci. Adv.* **3**, e1701079 (2017).
10. L.-G. Mattsson, E. Jenelius, Vulnerability and resilience of transport systems—A discussion of recent research. *Transp. Res. Part A Policy Pract.* **81**, 16–34 (2015).
11. E. Jenelius, Redundancy importance: Links as rerouting alternatives during road network disruptions. *Procedia Eng.* **3**, 129–137 (2010).
12. X. Xu, A. Chen, S. Jansuwan, K. Heaslip, C. Yang, Modeling transportation network redundancy. *Transp. Res. Procedia* **9**, 283–302 (2015).
13. H. Demirel, M. Kompil, F. Nemry, A framework to analyze the vulnerability of European road networks due to sea-level rise (SLR) and sea storm surges. *Transp. Res. Part A Policy Pract.* **81**, 62–76 (2015).
14. A. Reggiani, P. Nijkamp, D. Lanzi, Transport resilience and vulnerability: The role of connectivity. *Transp. Res. Part A Policy Pract.* **81**, 4–15 (2015).
15. S. Weilant, A. Strong, B. M. Miller, *Incorporating Resilience into Transportation Planning and Assessment* (RAND Corporation, 2019).
16. S. A. Markolf, C. Hoehne, A. Fraser, M. V. Chester, B. S. Underwood, Transportation resilience to climate change and extreme weather events – Beyond risk and robustness. *Transp Policy* **74**, 174–186 (2019).
17. A. Pisarski, *Commuting in America III: The Third National Report on Commuting Patterns and Trends* (Transportation Research Board, 2006), vol. 550.

18. United States Census Bureau, Longitudinal Employer-Household Dynamics Origin Destination Employment Statistics—Geodatabase Format: 2015 (2015); https://lehd.ces.census.gov/data/.
19. P. Suarez, W. Anderson, V. Mahal, T. R. Lakshmanan, Impacts of flooding and climate change on urban transportation: A systemwide performance assessment of the Boston Metro Area. *Transp. Res. D Transp. Environ.* **10**, 231–244 (2005).
20. P. Wang, T. Hunter, A. M. Bayen, K. Schechtner, M. C. González, Understanding road usage patterns in urban areas. *Sci. Rep.* **2**, 1001 (2012).
21. M. Chen, A. S. Alfa, A network design algorithm using a stochastic incremental traffic assignment approach. *Transp. Sci.* **25**, 215–224 (1991).
22. Metropolitan Transportation Commission/Association of Bay Area Governments (MTC/ABAG), Regional Road Network—Shapefile Format: 2015 (2017); http://analytics.mtc.ca.gov/foswiki/bin/view/Main/DataRepository.
23. G. Erhardt, D. Ory, A. Sarvepalli, J. Freedman, J. Hood, B. Stabler, MTC's Travel Model One: Applications of an Activity-Based Model in its First Year, paper presented at the *5th Transportation Research Board Innovations in Travel Modeling Conference, Tampa, Florida*. Originally presented at and winner of Best Presentation award at Futura 2011: Citilabs Annual International Users Conference, Palm Springs, CA, (2012).
24. United States Census Bureau, American Community 1-Year Survey—Geodatabase Format: 2016 (2016).
25. United States Census Bureau, TIGER/Line Shapefile Products—Shapefile Format: 2018 (2015); www.census.gov/geographies/mapping-files/time-series/geo/tiger-line-file.html.
26. National Research Council, *Sea-Level Rise for the Coasts of California, Oregon, and Washington: Past, Present, and Future* (The National Academis Press, 2012).
27. California Natural Resources Agency, California Ocean Protection Council, State of California Rise Guidance—2018 Update (2018); www.opc.ca.gov/updating-californias-sea-level-rise-guidance/.
28. National Oceanic and Atmospheric Administration, Turn Around Don't Drown, *National Weather Service*; www.weather.gov/safety/flood-turn-around-dont-drown.
29. M. Pregnolato, A. Ford, S. M. Wilkinson, R. J. Dawson, The impact of flooding on road transport: A depth-disruption function. *Transp. Res. D Transp Environ.* **55**, 67–81 (2017).
30. California Department of Transportation (Caltrans), California Road Elevation Measurement—Shapefile Format: 2016 (2016).
31. D. J. Tyler, Topobathymetric Model for the San Francisco Bay, California, 1929 to 2017: U.S. Geological Survey Data Release (2018); https://doi.org/10.5066/F7736Q34.
32. J. Suh, A. T. Siwe, S. M. Madanat, Transportation infrastructure protection planning against sea level rise: Analysis using operational landscape units. *J. Infrastruct. Syst.* **25**, 04019024 (2019).
33. A. Colsaet, Y. Laurans, H. Levrel, What drives land take and urban land expansion? A systematic review. *Land Use Policy* **79**, 339–349 (2018).
34. C. Benner, A. Karner, Low-wage jobs-housing fit: Identifying locations of affordable housing shortages. *Urban Geogr.* **37**, 883–903 (2016).
35. A. Mann, T. Luo, Crash and reboot: Silicon Valley high-tech employment and wages, 2000–08. *Mon. Labor Rev.* **141**, 59–73 (2010).
36. Metropolitan Transportation Commission, Association of Bay Area Governments, Plan Bay Area 2040 (2017); http://2040.planbayarea.org/reports.
37. P. Crucitti, V. Latora, S. Porta, Centrality measures in spatial networks of urban streets. *Phys. Rev. E.* **73**, 036125 (2006).
38. A. Kermanshah, S. Derrible, Robustness of road systems to extreme flooding: Using elements of GIS, travel demand, and network science. *Nat. Hazards* **86**, 151–164 (2017).
39. J. Peponis, S. Bafna, Z. Zhang, The connectivity of streets: Reach and directional distance. *Environ. Plann. B Plann. Des.* **35**, 881–901 (2008).
40. M. Mak, E. Harris, M. Lightner, J. Vandever, K. May, *San Francisco Bay Tidal Datums and Extreme Tides Study*, Prepared for the Federal Emergency Management Agency by AECOM: Oakland, CA, USA (2016); https://www.adaptingtorisingtides.org/wp-content/uploads/2016/05/20160429.SFBay_Tidal-Datums_and_Extreme_Tides_Study.FINAL_.pdf.
41. D. Marcy, B. William, K. Dragonoz, B. Hadley, C. Haynes, N. Herold, J. McCombs, M. Pendleton, S. Ryan, K. Schmid, M. Sutherland, K. Waters, New Mapping Tool and Techniques or Visualizing Sea Level Rise and Coastal Flooding Impacts, in *Proceedings of the 2011 Solutions to Coastal Disasters Conference*, Anchorage, AK, June 2011.

Acknowledgments: Our work is the product of the Stanford Future Bay Initiative, a research-education-practice-partnership committed to coproduction of actionable intelligence with San Francisco Bay Area communities, to shape a more equitable, resilient, and sustainable urban future. This research emerged out of a year-long service learning class in the 2017–2018 academic year. We particularly acknowledge the contributions of A. Mariwala and J. Zhao. We thank M. Miller for developing the publicly available base code for the incremental traffic assignment algorithm and for providing a layout for assessing hazard-related traffic disruption. We thank J. Baker for insightful comments, in-depth discussions, and guidance on the details of the traffic model for this paper. We also thank G. Bhattacharjee for initial conversations associated with this project. We thank our community partners who engaged with the group over the 2017–2018 academic year, particularly J. Sharma, H. Papendick, D. Forsell, and J. Vo. We thank the members of MTC/ABAG, particularly M. Germeraad and L. Zorn, for comments on traffic modeling. We thank the members of Caltrans, particularly R. Fahey and R. Sherrick, for correspondence and for providing California road elevation datasets. **Funding:** This research was supported primarily by the UPS Endowment Fund and Stanford's Bill Lane Center for the American West. This research was partially inspired and funded by the NSF through the Office of Polar Programs awards PLR-1744758 and PLR-1739027. I.G.K. was supported by the Stanford Graduate Fellowship. We also acknowledge support from the following units that are part of, or affiliated with, Stanford University: the Haas Center for Public Service; the School of Earth, Energy and Environmental Sciences; the Department of Civil and Environmental Engineering; the Institute for Computational and Mathematical Engineering; the Center for Sustainable Development and Global Competitiveness; Stanford Professionals in Real Estate; the Dawe family; and the Woods Institute for the Environment. **Author contributions:** I.G.K. developed the model. Y.M., I.A.B., and K.A.S. validated the model results. I.G.K. and K.A.S. interpreted and analyzed the model results. I.G.K., K.A.S., and J.S. wrote the paper with input from I.A.B., Y.M., L.O., and D.O. I.G.K. and K.A.S. developed the figures for the manuscript. **Competing interests:** The authors declare that they have no competing interests. **Data and materials availability:** All data needed to evaluate the conclusions in the paper are present in the paper and/or the Supplementary Materials. The code for the traffic simulation and analysis is available at http://zapad.stanford.edu/sigma/flood-related-traffic-disruption. Additional data related to this paper may be requested from the authors.

Submitted 18 November 2019
Accepted 18 June 2020
Published 5 August 2020
10.1126/sciadv.aba2423

Citation: I. G. Kasmalkar, K. A. Serafin, Y. Miao, I. A. Bick, L. Ortolano, D. Ouyang, J. Suckale, When floods hit the road: Resilience to flood-related traffic disruption in the San Francisco Bay Area and beyond. *Sci. Adv.* **6**, eaba2423 (2020).